

Dissipative dynamics of an entangled three-qubit system via non-Hermitian Hamiltonian: Its correspondence with Markovian and non-Markovian regimes

M Rastegarzadeh and M K Tavassoly

Citation: Chin. Phys. B, 2021, 30 (**3**): 034205. DOI: 10.1088/1674-1056/abc2c3
Journal homepage: http://cpb.iphy.ac.cn; http://iopscience.iop.org/cpb

What follows is a list of articles you may be interested in

Deterministic nondestructive state analysis for polarization-spatial-time-bin hyperentanglement with cross-Kerr nonlinearity

Hui-Rong Zhang(张辉荣), Peng Wang(王鹏), Chang-Qi Yu(于长琦), and Bao-Cang Ren(任宝藏)
Chin. Phys. B, 2021, 30 (**3**): 030304. DOI: 10.1088/1674-1056/abd7d5

Majorana stellar representation for mixed-spin (*s*, 1/2) systems

Yu-Guo Su(苏玉国), Fei Yao(姚飞), Hong-Bin Liang(梁宏宾), Yan-Ming Che(车彦明), Li-Bin Fu(傅立斌), and Xiao-Guang Wang(王晓光)
Chin. Phys. B, 2021, 30 (**3**): 030303. DOI: 10.1088/1674-1056/abc2bc

Quantifying entanglement in terms of an operational way

Deng-Hui Yu(于登辉) and Chang-Shui Yu(于长水)
Chin. Phys. B, 2021, 30 (**2**): 020302. DOI: 10.1088/1674-1056/abc157

Quantum to classical transition induced by a classically small influence

Wen-Lei Zhao(赵文垒), Quanlin Jie(揭泉林)
Chin. Phys. B, 2020, 29 (**8**): 080302. DOI: 10.1088/1674-1056/ab8a3a

Detection and quantification of entanglement with measurement-device-independent and universal entanglement witness

Zhi-Jin Ke(柯芝锦), Yi-Tao Wang(王轶韬), Shang Yu(俞上), Wei Liu(刘伟), Yu Meng(孟雨), Zhi-Peng Li(李志鹏), Hang Wang(汪航), Qiang Li(李强), Jin-Shi Xu(许金时), Ya Xiao(肖芽), Jian-Shun Tang(唐建顺), Chuan-Feng Li(李传锋), Guang-Can Guo(郭光灿)
Chin. Phys. B, 2020, 29 (**8**): 080301. DOI: 10.1088/1674-1056/ab9288

Dissipative dynamics of an entangled three-qubit system via non-Hermitian Hamiltonian: Its correspondence with Markovian and non-Markovian regimes

M Rastegarzadeh and M K Tavassoly†

Laser and Optics Group, Faculty of Physics, Yazd University, Yazd 89195-741, *Iran*

(Received 14 July 2020; revised manuscript received 30 September 2020; accepted manuscript online 20 October 2020)

We investigate an entangled three-qubit system in which only one of the qubits experiences the decoherence effect by considering a non-Hermitian Hamiltonian, while the other two qubits are isolated, i.e., do not interact with environment, directly. Then, the time evolution of the density matrix (for the pure as well as mixed initial density matrix) and the corresponding reduced density matrices are obtained, by which we are able to utilize the dissipative non-Hermitian Hamiltonian model with Markovian and non-Markovian regimes via adjusting the strange of the non-Hermitian term of the total Hamiltonian of the under-considered system.

Keywords: non-Hermitian Hamiltonian, entanglement, concurrence measure, Markovian and non-Markovian regimes

PACS: 03.67.Mn, 03.65.Yz, 03.67.Bg **DOI:** 10.1088/1674-1056/abc2c3

1. Introduction

Quantum entanglement, as a marvellous phenomena in quantum optics and quantum mechanics, has been utilized in quantum information science and technologies.[1–5] The dissipation as a source of entanglement attenuation, which destroys quantum coherence, has been converted to the most important and ubiquitous topics in quantum optics of open quantum systems. Dissipative systems have been investigated with different approaches.[6–8] Among them we may refer to density operator (the Lindbland master equation), quantum jump and noise operator approach.[9] In the studies on the interaction of quantum optics systems with their environments, two main regimes are considered, known as Markovian and non-Markovian. The quantum Fisher information flow may be employed for distinguishing the Markovian and non-Markovian processes.[10,11] Moreover, in particular, the entanglement revives in the non-Markovian regime[9,12–15] and reduced exponentially in the Markovian regime.[16–18] In fact, even though Markovian dynamics includes a level of back reaction, it neglects the entanglement that arises between bodies and bath modes during the evolution. Although some works deal with this issue,[19] it is an attractive theoretical challenge to extend the obtained results under various conditions in the Markovian to the non-Markovian regime.[20]

Along the above-mentioned approaches, the non-Hermition Hamiltonian approach is a rather different method which has been frequently used in the literature deal with open quantum systems[21–26] and PT-symmetric systems.[27,28] Also, a few applications of non-Hermitian Hamiltonian in quantum optics have been established in Ref. [29]. According to the theory of quantum jump, whenever no detector click occurs, the system dynamics follows a non-unitary evolution (which governs via a suitable non-Hermitian Hamiltonian[7]). For further usefulness of non-Hermitian operators in quantum optics studies, one may refer to Ref. [30]. Related to the latter approach, in Ref. [21], non-Hermitian Hamiltonian for a modulated Jaynes–Cummings model has been studied. The entropy of "single-qubit" is evaluated by considering a general non-Hermitian Hamiltonian.[22–24] Also, the authors in Ref. [25] investigated the evolution of quantum (von Neumann) entropy and entropic uncertainty of an entangled "two-qubit" system in which only one of the two qubits is affected by the environment described via a non-Hermitian Hamiltonian.

Moreover, as is found in the literature, extending two-partite systems to three- and more-partite systems is of enough interest for their usefulness applications. For instance, quantum teleportation protocols, based on three-qubit (or in general multi-qubit) entangled states, are widely used in order to construct quantum networks in the theoretical[31–34] and practical[35–37] researches, especially for their applications in the content of weak measurement and quantum measurement reversal.[38–40] As an example, the extension of entanglement in superconducting circuits, which has been so far limited to two qubits, to three, eight and ten qubits has been achieved among spins, ions and photons, respectively.[41]

Motivating by the above-mentioned facts, in the present work we study the entanglement dynamics of an entangled "three-qubit" system in the presence of dissipation via extend-

†Corresponding author. E-mail: mktavassoly@yazd.ac.ir

© 2021 Chinese Physical Society and IOP Publishing Ltd

ing the presented approach in Refs. [25,26], wherein a two-qubit system is considered (one of them is interacted with its environment and the other one is isolated), and a non-Hermitian Hamiltonian is used. In detail, we assume three entangled qubits, where only one of them interacts with the environment via a non-Hermitian Hamiltonian and the other two qubits have been isolated. Our aim is to investigate the entanglement time behavior of each pair of qubits. To achieve our purpose, we obtain the temporal evolution of the density matrix of the entire system via applying time evolution operator on the two initial states, in the cases of pure and mixed initial density matrices. Then, we calculate the reduced density matrix associated with all possible qubit pairs of the three qubits. In the continuation, we evaluate the dynamics of entanglement of the three possible qubit pairs via the concurrence measure for deferent initial conditions, either with pure or mixed initial states. As a further interesting result of this work, we will establish a suitable correspondence between the considered dissipative model with the Markovian and non-Markovian regimes by introducing a critical value for the dissipative parameter in the considered non-Hermitian Hamiltonian approach.

The rest of the paper is organized as follows: In Section 2, we present our model and investigate its evolution. In Section 3, we investigate the evolution of entanglement among three considered qubits when the system is initially prepared in pure as well as in mixed states. Finally, we provide our concluding remarks.

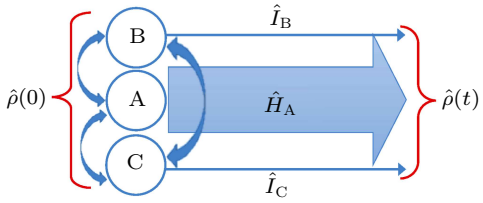


Fig. 1. Diagram of the entangled three-qubit system under the influence of environment.

2. The model and its evolution

We assume an entangled three-qubit system where the qubit A, with ground (excited) states $|0\rangle_{\rm A}$ ($|1\rangle_{\rm A}$) experiences a local environmental effect described by a non-Hermitian Hamiltonian, while the other two qubits B and C, with ground (excited) states $|0\rangle_{\rm B}$ ($|1\rangle_{\rm B}$) and $|0\rangle_{\rm C}$ ($|1\rangle_{\rm C}$), are isolated (see Fig. 1). The general form of the non-Hermitian Hamiltonian $\hat{H}_A$ is written as

$$\hat{H}_{\rm A} = \hat{H}_+ - {\rm i}\hat{\Gamma}, \tag{1}$$

where both $\hat{H}_+ = \hat{H}_+^{\dagger}$ and $\hat{\Gamma} = \hat{\Gamma}^{\dagger}$ are Hermitian. In particular, Hamiltonian (1) may be defined in the following form ($\hbar = 1$),

$$\hat{H}_{\rm A} = -\Delta\hat{\sigma}_x^{\rm A} - {\rm i}\gamma\hat{\sigma}_z^{\rm A}, \tag{2}$$

where the real values Δ and γ describe the strength of Hermitian and non-Hermitian parts of Hamiltonian, respectively. Also, $\hat{\sigma}_x^{\rm A}$ and $\hat{\sigma}_z^{\rm A}$ are Pauli matrices for qubit A. Now, we are going to determine the time-dependent density operator of the system by applying the time evolution operator $\hat{U}(t) = \hat{U}_{\rm A}\otimes\hat{I}_{\rm B}\otimes\hat{I}_{\rm C}$ on the initial density operator as follows:

$$\hat{\rho}(t) = \hat{U}(t)\hat{\rho}(0)\hat{U}^{\dagger}(t). \tag{3}$$

Note that $\hat{\rho}(t)$ is not trace preserved here due to the non-Hermitian Hamiltonian of system, while observers have to measure the quantum system in conventional quantum world. Thus, $\hat{\rho}(t)$ should be normalized as

$$\tilde{\hat{\rho}}(t) = \frac{\hat{\rho}(t)}{{\rm Tr}\hat{\rho}(t)}. \tag{4}$$

By straightforward calculations, we achieve the matrix corresponding to the time-evolution operator of qubit A as follows:

$$\hat{U}_{\rm A}(t) = \begin{pmatrix} U_{11}(t) & U_{12}(t) \\ U_{21}(t) & U_{22}(t) \end{pmatrix}, \tag{5}$$

with elements

$$\begin{aligned} U_{11}(t) &= \cosh(\mu\tau) - \frac{\tilde{\gamma}}{\mu}\sinh(\mu\tau), \\ U_{22}(t) &= \cosh(\mu\tau) + \frac{\tilde{\gamma}}{\mu}\sinh(\mu\tau), \\ U_{12}(t) &= U_{21}(t) = \frac{\rm i}{\mu}\sinh(\mu\tau). \end{aligned} \tag{6}$$

For simplicity, we use the notations $\tau = \Delta t$, $\tilde{\gamma} = \gamma/\Delta$ and $\mu = \sqrt{\tilde{\gamma}^2 - 1}$.

3. Entanglement of the system in the absence and presence of dissipation

3.1. The concurrence for the initial pure state

At this stage, we assume that the three-qubit system is initially prepared in two pure states, i.e., the generalized Schmidt decomposition as Werner state (W-state)[42] as well as the generalized Greenberger–Horne–Zeilinger (GHZ) state[43,44] as follows:

$$\begin{aligned} |\Psi(0)\rangle_{\rm W} &= a|1\rangle_{\rm A}|0\rangle_{\rm B}|0\rangle_{\rm C} + b|0\rangle_{\rm A}|1\rangle_{\rm B}|0\rangle_{\rm C} \\ &\quad + c|0\rangle_{\rm A}|0\rangle_{\rm B}|1\rangle_{\rm C}, \end{aligned} \tag{7}$$

$$\begin{aligned} |\Psi(0)\rangle_{\rm G} &= \lambda_0|0\rangle_{\rm A}|0\rangle_{\rm B}|0\rangle_{\rm C} + \lambda_1 {\rm e}^{{\rm i}\phi}|1\rangle_{\rm A}|0\rangle_{\rm B}|0\rangle_{\rm C} \\ &\quad + \lambda_2|1\rangle_{\rm A}|0\rangle_{\rm B}|1\rangle_{\rm C} + \lambda_3|1\rangle_{\rm A}|1\rangle_{\rm B}|0\rangle_{\rm C} \\ &\quad + \lambda_4|1\rangle_{\rm A}|1\rangle_{\rm B}|1\rangle_{\rm C}, \end{aligned} \tag{8}$$

where the state ket $|0\rangle_i$ ($|1\rangle_i$) is denoted for the ground (excited) state of the i-th qubit, $i = {\rm A,B,C}$. The assumed (real)

coefficients must satisfy the normalization relations $a^2+b^2+c^2=1$ and $\sum_{j=0}^{4}\lambda_j^2=1$ with $0\le\phi\le\pi$.

Therefore, we have

$$\hat{\rho}_{\mathrm{W(G)}}(0)=|\Psi(0)\rangle_{\mathrm{W(G)}}\langle\Psi(0)|. \tag{9}$$

Using Eqs. (3), (4), (5), (7) and (8), and after some lengthy calculations, the explicit form of the density operator of the system can be obtained. As a result, the reduced density matrices can be calculated by

$$\begin{aligned}&\hat{\rho}_{\mathrm{red}}^{\mathrm{AB}}(t)=\mathrm{tr_C}(\tilde{\hat{\rho}}(t)),\quad \hat{\rho}_{\mathrm{red}}^{\mathrm{AC}}(t)=\mathrm{tr_B}(\tilde{\hat{\rho}}(t)),\\ &\hat{\rho}_{\mathrm{red}}^{\mathrm{BC}}(t)=\mathrm{tr_A}(\tilde{\hat{\rho}}(t)).\end{aligned} \tag{10}$$

Here, we represent only one of the above reduced density matrices (ρ^{AB}) for the above introduced initial states in Eqs. (7) and (8):

$$\hat{\rho}_{\mathrm{red}}^{\mathrm{AB}}=\frac{1}{\mathcal{N}_{\mathrm{W(G)}}(t)}\begin{pmatrix}\rho_{11}^{\mathrm{AB}}&\rho_{12}^{\mathrm{AB}}&\rho_{13}^{\mathrm{AB}}&\rho_{14}^{\mathrm{AB}}\\ \rho_{21}^{\mathrm{AB}}&\rho_{22}^{\mathrm{AB}}&\rho_{23}^{\mathrm{AB}}&\rho_{24}^{\mathrm{AB}}\\ \rho_{31}^{\mathrm{AB}}&\rho_{32}^{\mathrm{AB}}&\rho_{33}^{\mathrm{AB}}&\rho_{34}^{\mathrm{AB}}\\ \rho_{41}^{\mathrm{AB}}&\rho_{42}^{\mathrm{AB}}&\rho_{43}^{\mathrm{AB}}&\rho_{44}^{\mathrm{AB}}\end{pmatrix}, \tag{11}$$

where $\mathcal{N}_{\mathrm{W(G)}}(t)$ is the normalization factor that reads

$$\begin{aligned}\mathcal{N}_{\mathrm{W}}(t)&=(b^2+c^2)\left[U_{22}^2(t)-U_{12}^2(t)\right]\\ &\quad+a^2\left[U_{11}^2(t)-U_{12}^2(t)\right],\end{aligned} \tag{12}$$

$$\begin{aligned}\mathcal{N}_{\mathrm{G}}(t)&=\lambda_0^2\left(U_{22}^2(t)-U_{12}^2(t)\right)+\left(\lambda_1^2+\lambda_2^2+\lambda_3^2+\lambda_4^2\right)\\ &\quad\times\left(U_{11}^2(t)-U_{12}^2(t)\right)\\ &\quad+2\mathrm{i}\sin\phi\lambda_0\lambda_1U_{12}(t)\big(U_{22}(t)-U_{11}(t)\big).\end{aligned} \tag{13}$$

The matrix elements in Eq. (11) for the initial W-state are given by

$$\begin{aligned}&\rho_{11}^{\mathrm{AB}}=-b^2U_{12}^2(t),\quad \rho_{22}^{\mathrm{AB}}=b^2U_{22}^2(t),\\ &\rho_{33}^{\mathrm{AB}}=a^2U_{11}^2(t)-c^2U_{12}^2(t),\quad \rho_{44}^{\mathrm{AB}}=c^2U_{22}^2(t)-a^2U_{12}^2(t),\\ &\rho_{12}^{\mathrm{AB}}=-\rho_{21}^{\mathrm{AB}}=b^2U_{12}(t)U_{22}(t),\\ &\rho_{13}^{\mathrm{AB}}=-\rho_{31}^{\mathrm{AB}}=abU_{11}(t)U_{12}(t),\\ &\rho_{14}^{\mathrm{AB}}=\rho_{41}^{\mathrm{AB}}=-abU_{12}^2(t),\\ &\rho_{23}^{\mathrm{AB}}=\rho_{32}^{\mathrm{AB}}=abU_{11}(t)U_{22}(t),\\ &\rho_{24}^{\mathrm{AB}}=-\rho_{42}^{\mathrm{AB}}=-abU_{12}(t)U_{22}(t),\\ &\rho_{34}^{\mathrm{AB}}=-\rho_{43}^{\mathrm{AB}}=-a^2U_{11}(t)U_{12}(t)+c^2U_{22}(t)U_{12}(t).\end{aligned} \tag{14}$$

Such matrix elements for the initial GHZ-state are represented in appendix A. Now, due to the important role of entanglement in quantum science and technologies, we pay our attention to the entanglement between the qubits A and B via the concurrence measure. This quantity is defined as[45]

$$C(t)=\max\{0,\sqrt{e_1}-\sqrt{e_2}-\sqrt{e}_3-\sqrt{e}_4\}, \tag{15}$$

where e_i $(i=1,2,3,4)$ are the eigenvalues of the matrix $\hat{\rho}_{\mathrm{red}}^{\mathrm{AB}}(\hat{\sigma}_y^{\mathrm{A}}\otimes\hat{\sigma}_y^{\mathrm{B}})(\hat{\rho}_{\mathrm{red}}^{\mathrm{AB}})^*(\hat{\sigma}_y^{\mathrm{A}}\otimes\hat{\sigma}_y^{\mathrm{B}})$ in decreasing order with $(\hat{\rho}_{\mathrm{red}}^{\mathrm{AB}})^*$ as the complex conjugate of $\hat{\rho}_{\mathrm{red}}^{\mathrm{AB}}$. Also, $\hat{\sigma}_y^{\mathrm{A}}$ and $\hat{\sigma}_y^{\mathrm{B}}$ are the usual y Pauli matrices for the qubits A and B, respectively. In this way, the concurrence of qubit pair AB that is initially prepared in W-state can be obtained as follows:

$$C_{\mathrm{W}}^{\mathrm{AB}}(t)=\left|\frac{2}{\mathcal{N}_{\mathrm{W}}(t)}ab\left[U_{12}^2(t)-U_{11}(t)U_{22}(t)\right]\right|. \tag{16}$$

Similarly, by considering the same initial state for the other two pairs of qubits, i.e., AC and BC, one arrives at

$$C_{\mathrm{W}}^{\mathrm{AC}}(t)=\left|\frac{2}{\mathcal{N}_{\mathrm{W}}(t)}ac\left[U_{12}^2(t)-U_{11}(t)U_{22}(t)\right]\right|, \tag{17}$$

$$C_{\mathrm{W}}^{\mathrm{BC}}(t)=\left|\frac{2}{\mathcal{N}_{\mathrm{W}}(t)}bc\left[U_{12}^2(t)-U_{22}^2(t)\right]\right|. \tag{18}$$

Also, we have obtained the concurrence measure for all three pairs of qubits AB, AC and BC in the following form, when we consider the GHZ-state (8) as the initial state of the system,

$$\begin{aligned}C_{\mathrm{G}}^{\mathrm{AB}}(t)&=\frac{\lambda_0}{\mathcal{N}_{\mathrm{G}}(t)}\sqrt{\left(2\lambda_3^2+\lambda_4^2\right)\left(U_{12}^2(t)-U_{11}(t)U_{22}(t)\right)^2+2\sqrt{\lambda_3^2\left(\lambda_3^2+\lambda_4^2\right)\left(U_{12}^2(t)-U_{11}(t)U_{22}(t)\right)^4}}\\ &\quad-\sqrt{\left(2\lambda_3^2+\lambda_4^2\right)\left(U_{12}^2(t)-U_{11}(t)U_{22}(t)\right)^2-2\sqrt{\lambda_3^2\left(\lambda_3^2+\lambda_4^2\right)\left(U_{12}^2(t)-U_{11}(t)U_{22}(t)\right)^4}},\end{aligned} \tag{19}$$

$$\begin{aligned}C_{\mathrm{G}}^{\mathrm{AC}}(t)&=\frac{\lambda_0}{\mathcal{N}_{\mathrm{G}}(t)}\sqrt{\left(2\lambda_2^2+\lambda_4^2\right)\left(U_{12}^2(t)-U_{11}(t)U_{22}(t)\right)^2+2\sqrt{\lambda_2^2\left(\lambda_2^2+\lambda_4^2\right)\left(U_{12}^2(t)-U_{11}(t)U_{22}(t)\right)^4}}\\ &\quad-\sqrt{\left(2\lambda_2^2+\lambda_4^2\right)\left(U_{12}^2(t)-U_{11}(t)U_{22}(t)\right)^2-2\sqrt{\lambda_2^2\left(\lambda_2^2+\lambda_4^2\right)\left(U_{12}^2(t)-U_{11}(t)U_{22}(t)\right)^4}},\end{aligned} \tag{20}$$

$$\begin{aligned}C_{\mathrm{G}}^{\mathrm{BC}}(t)&=\frac{1}{\mathcal{N}_{\mathrm{G}}(t)}\left(\sqrt{\eta(t)+\sqrt{\eta^2(t)-\frac{1}{4}\lambda_0^4\lambda_4^4(U_{12}^2(t)-U_{11}(t)U_{22}(t))^4}}\right)\\ &\quad-\left(\sqrt{\eta(t)-\sqrt{\eta^2(t)-\frac{1}{4}\lambda_0^4\lambda_4^4(U_{12}^2(t)-U_{11}(t)U_{22}(t))^4}}\right),\end{aligned} \tag{21}$$

where we have defined

$$\begin{aligned}\eta(t) \;=\; & 2\left(\lambda_2^2\lambda_3^2 - 2\lambda_1\lambda_2\lambda_3\lambda_4\cos\phi + \lambda_0\lambda_1\lambda_4^2\right) \\ & \times \left(U_{11}^2(t) - U_{12}^2(t)\right)^2 - 4\mathrm{i}\lambda_0\lambda_1\lambda_4^2\sin\phi(U_{11}^2(t) \\ & - U_{12}^2(t))((U_{11}(t) - U_{22}(t))) \\ & - \lambda_0^2\lambda_4^2\big(U_{12}^2(t)\big(2\big(U_{11}^2(t) + U_{22}^2(t) \\ & - U_{11}(t)U_{22}(t) - U_{12}^2(t)\big) - U_{11}^2(t)U_{22}^2(t)\big)\big). \quad (22)\end{aligned}$$

Note that $\{U_{ij}\}$ in Eqs. (12)–(14) and (16)–(22) have been introduced in Eq. (6). Using Eqs. (16)–(18) the concurrences measured, corresponding to the qubit pairs AB, AC and BC for the initial W-state against the scaled time $\tau = \Delta t$ and for different values of non-Hermitian (dissipation) parameter $\tilde{\gamma}$, have been shown in Fig. 2. Also, we use Eqs. (19)–(21) in Fig. 3 for the initial GHZ-state. In addition, we have plotted the concurrences for the symmetrical and asymmetrical initial conditions respectively in left and right curves in Figs. 2 and 3. Considering the symmetrical initial conditions $a = b = c$ and $\lambda_0 = \lambda_1 = \lambda_2 = \lambda_3 = \lambda_4$, respectively, for W- and GHZ-state, the concurrences of the pairs of qubits AC and AB are the same (compare Eqs. (16) and (19) with Eqs. (17) and (20), respectively). It is interesting to notice that the initial state with no initial entanglement between qubit A and the entangled qubits B and C, which can be obtained by setting $a = 0$ in Eq. (7), still results in the time evolution of entanglement between B and C. This may be observed via the relations (12) and (18). By referring to the curves (plotted in Figs. 2 and 3) one may find that, as is usually expected, in the absence of dissipation, the concurrence of pairs of qubits is preserved and therefore, the entanglement between qubits is invariant as time is passed. However, in the presence of dissipation, the amount of entanglement varies as time goes on. In particular, for $\tilde{\gamma} < 1$ we observe a few oscillations in all subsystems conforming the entanglement behavior within the non-Markovian regimes.[46–49] However, for dissipation values in the range $\tilde{\gamma} > 1$, the entanglement degree in the two pairs of qubits AB and AC drops out to zero, without any oscillation, i.e., such behavior is seen in the Markovian regimes.[50] Interestingly, again for $\tilde{\gamma} > 1$ in the qubit pair BC the entanglement grows to some stable values more than the initial values, while we assume that the two qubits B and C are initially isolated (see Figs. 2(e), 2(f), 3(e) and 3(f)).

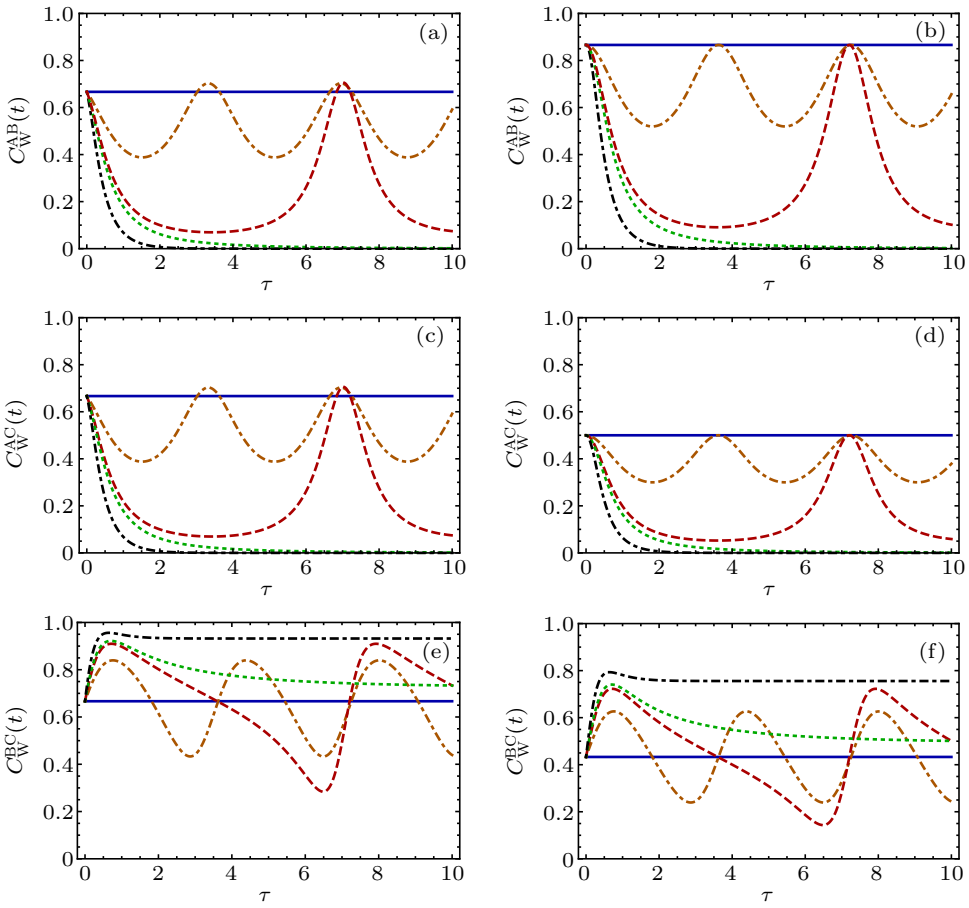


Fig. 2. The concurrence of the qubit pairs against scaled time $\tau = \Delta t$ for the initial W-state in the subspecies [(a), (b)], [(c). (d)], and [(e), (f)] for the pairs AB, AC and BC, respectively. We plot the left curves for the symmetrical initial conditions $a = b = c = \sqrt{1/3}$ and the right curves for the asymmetrical conditions $a = \sqrt{1/2}$, $b = \sqrt{3/8}$, $c = \sqrt{1/8}$. Furthermore, we consider different values $\tilde{\gamma} = 0$ (continuous blue line), $\tilde{\gamma} = 0.5$ (dot-dashed orange line), $\tilde{\gamma} = 0.9$ (dashed red line), $\tilde{\gamma} = 1.01$ (dotted green line) and $\tilde{\gamma} = 1.5$ (black dot-dashed line).

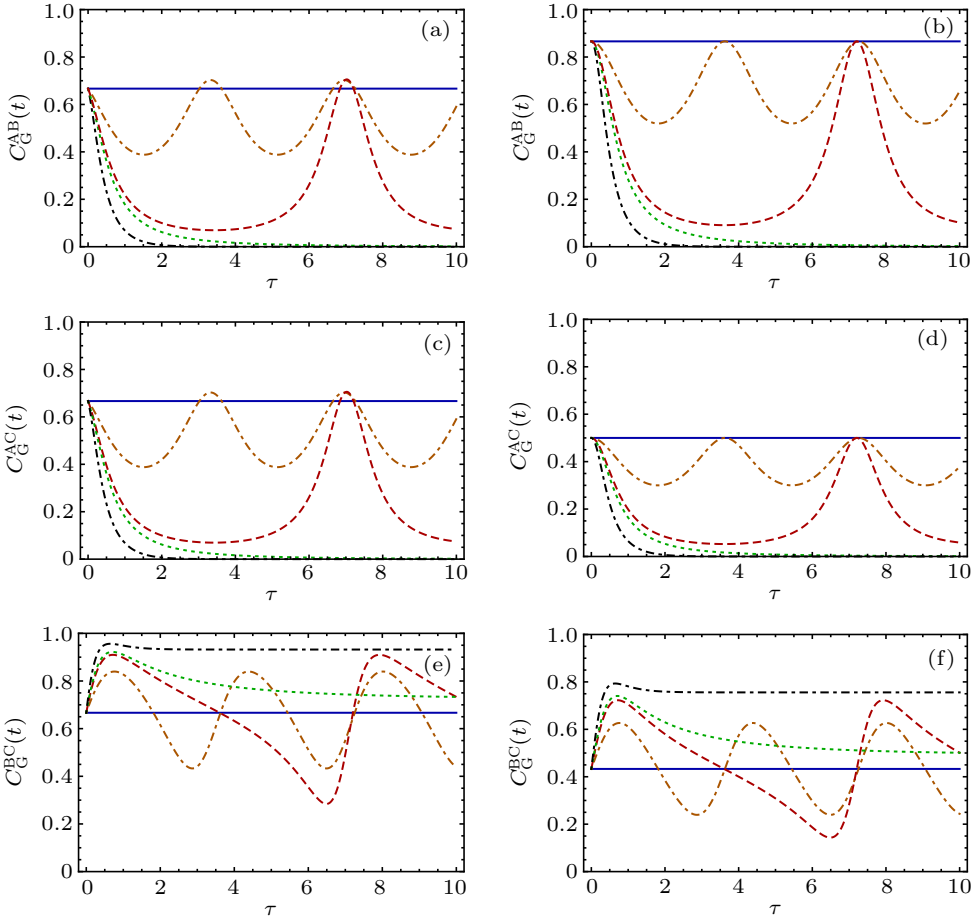


Fig. 3. The concurrence of the qubit pairs against scaled time $\tau = \Delta t$ for the initial GHZ-state in the subspecies [(a), (b)], [(c), (d)], and [(e), (f)] for the pairs AB, AC and BC, respectively. We plot the left curves for the symmetrical initial conditions $\lambda_0 = \lambda_1 = \lambda_2 = \lambda_3 = \lambda_4 = 1/\sqrt{5}$ and the right curves for the asymmetrical conditions $\lambda_0 = \sqrt{0.1}$, $\lambda_1 = \sqrt{0.3}$, $\lambda_2 = \sqrt{0.1}$, $\lambda_3 = \sqrt{0.3}$, $\lambda_4 = \sqrt{0.2}$. Furthermore, we consider $\phi = \pi/2$ and the values of $\tilde{\gamma}$ as same as those in Fig. 2.

3.2. The concurrence for the initial mixed state

Here we suppose that the initial state of the system is prepared in ensembles of states $|\Psi\rangle_1$ and $|\Psi\rangle_2$ with classical probabilities w_1 and w_2, respectively. Thus, the density operator describing the entire system can be written as

$$\hat{\rho}(0) = w_1 |\Psi_1\rangle\langle\Psi_1| + w_2 |\Psi_2\rangle\langle\Psi_2|, \tag{23}$$

$$|\Psi_1\rangle = [a_1 |1\rangle_A |0\rangle_B + b_1 |0\rangle_A |1\rangle_B](\sin\alpha_1 |1\rangle_C + e^{i\phi_1}\cos\alpha_1 |0\rangle_C), \tag{24}$$

$$|\Psi_2\rangle = [a_2 |1\rangle_A |0\rangle_C + b_2 |0\rangle_A |1\rangle_C](\sin\alpha_2 |1\rangle_B + e^{i\phi_2}\cos\alpha_2 |0\rangle_B), \tag{25}$$

where $a_i^2 + b_i^2 = 1$ $(i = 1, 2)$. As is seen, in $|\Psi_1\rangle$ the qubits A and B are in Bell-like states separable from qubit C, while in $|\Psi_2\rangle$ A and C are in Bell-like state separable from qubit B. By a straightforward calculations similar to subsection 3.1. Following Eqs. (3), (4), (5), (9) and (10), we may obtain the reduced density matrices $\rho_{red}^{AB}(t)$, $\rho_{red}^{AC}(t)$ and $\rho_{red}^{BC}(t)$ (as an example see appendix A for $\rho_{red}^{AB}(t)$). From Eq. (15), the concurrence of the qubit pair AB can be deduced as follows:

$$C^{AB}(t) = \sqrt{\gamma_{AB}(t) + \sqrt{2\lambda_{AB}(t)}} - \sqrt{\gamma_{AB}(t) - \sqrt{2\lambda_{AB}(t)}}, \tag{26}$$

where

$$\gamma_{AB}(t) = \frac{w_1}{2\mathcal{N}^2(t)}\big[b_1{}^2a_2{}^2w_2 + a_1{}^2(4b_1{}^2w_1 + b_2{}^2w_2) + (b_1a_2 - a_1b_2)(b_1a_2 + a_1b_2)w_2\cos 2\alpha_2\big] \times \big(U_{12}^2(t) - U_{11}(t)U_{22}(t)\big)^2, \tag{27}$$

$$\lambda_{AB}(t) = \frac{a_1{}^2b_1{}^2w_1^3}{\mathcal{N}^4(t)}\big[b_1{}^2a_2{}^2w_2 + a_1{}^2(2b_1{}^2w_1 + b_2{}^2w_2) + (b_1a_2 - a_1b_2)(b_1a_2 + a_1b_2)w_2\cos 2\alpha_2\big] \times \big(U_{12}^2(t) - U_{11}(t)U_{22}(t)\big)^4, \tag{28}$$

with $\mathcal{N}(t)$ as the normalization as

$$\mathcal{N}(t) = \big(a_1{}^2w_1 + a_2{}^2w_2\big)U_{11}^2(t) - \big((a_1{}^2 + b_1{}^2)w_1 + (a_2{}^2 + b_2{}^2)w_2\big)U_{12}^2(t) + \big(b_1{}^2w_1 + b_2{}^2w_2\big)U_{22}^2(t). \tag{29}$$

Similarly, for the concurrence of the qubit pair AC one finds

$$C^{AC}(t) = \sqrt{\gamma_{AC}(t) + \sqrt{2\lambda_{AC}(t)}} - \sqrt{\gamma_{AC}(t) - \sqrt{2\lambda_{AC}(t)}}, \tag{30}$$

where

$$\gamma_{AC}(t) = \frac{w_2}{2\mathcal{N}^2(t)}[b_1{}^2a_2{}^2w_1 + b_2{}^2(a_1{}^2w_1 + 4a_2{}^2w_2)$$

$$+(-{b_1}^2{a_2}^2+{a_1}^2{b_2}^2)w_1\cos 2\alpha_1]$$
$$\times\left(U_{12}^2(t)-U_{11}(t)U_{22}(t)\right)^2, \quad (31)$$

$$\lambda_{\rm AC}(t) = \frac{{a_2}^2{b_2}^2w_2^3}{\mathcal{N}^4(t)}[{b_1}^2{a_2}^2w_1+{b_2}^2({a_1}^2w_1+2{a_2}^2w_2)$$
$$+(-{b_1}^2{a_2}^2+{a_1}^2{b_2}^2)w_1\cos 2\alpha_1]$$
$$\times\left(U_{12}^2(t)-U_{11}(t)U_{22}(t)\right)^4. \quad (32)$$

Furthermore, our calculations for the concurrence of the qubit pair BC lead to $C^{\rm BC}(t)=C^{\rm BC}(0)=0$. In detail, we would like to mention that in this case, in our calculation for concurrence $C^{\rm BC}$ considering the initial mixed state, two of the eigenvalues for the related matrix are the same. Thus, based on the concurrence relation (15), we achieve $C^{\rm BC}=0$, meaning that the qubits B and C are always separable. Furthermore, to determine our calculations, we re-investigate the entanglement of the two qubits B and C when they are initially prepared in a mixed state via the negativity measure and we have obtained the same conclusion with concurrence. Moreover, our numerical results for the concurrences (26) and (30) are respectively shown in Fig. 4 against the scaled time $\tau=\Delta t$ with the symmetrical initial values $a_1=b_1=a_2=b_2=\sqrt{1/2}$, $\alpha_1=\alpha_2=\pi/4$ in the left curves and with the asymmetrical initial values $a_1=\sqrt{2/3}$, $a_2=\sqrt{1/3}$, $b_1=\sqrt{7/8}$, $b_2=\sqrt{1/8}$, $\alpha_1=\pi/2$, $\alpha_2=\pi/4$ in the right curves. Also, we consider the values of probabilities as $w_1=w_2=0.5$, $\phi_1=\phi_2=\pi/2$ for different values of $\tilde{\gamma}$. Clearly, we can still deduce the same correspondence with the non-Markovian and Markovian regimes, depending on the values of dissipation parameter $\tilde{\gamma}$.

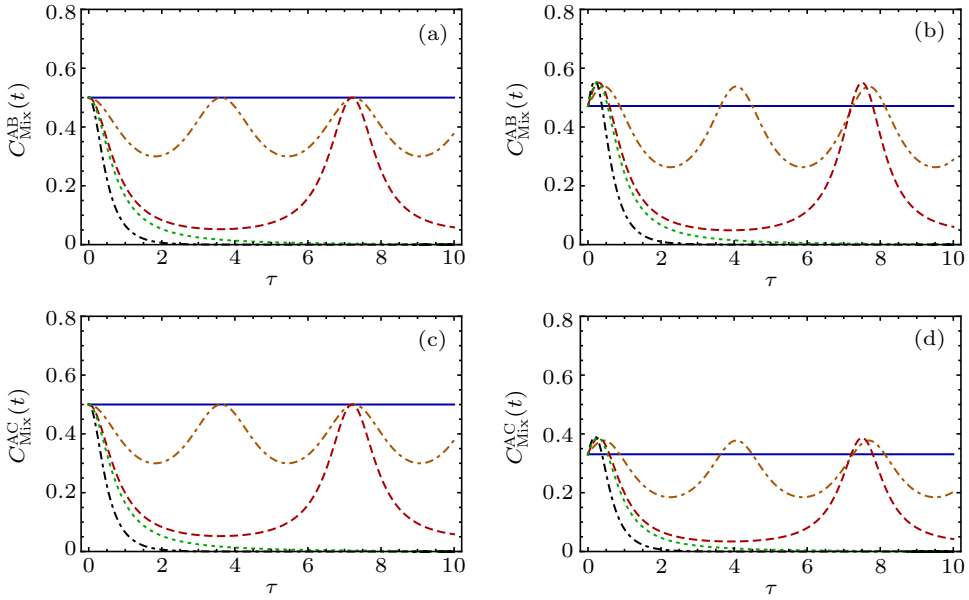


Fig. 4. The concurrence of the qubit pairs against scaled time $\tau=\Delta t$ for the initial mixed state in the subspecies [(a), (b)] and [(c), (d)], for the pairs AB and AC, respectively. We plot the left curves for the symmetrical initial conditions $a_1=a_2=b_1=b_2=1/\sqrt{2}$, $\alpha_1=\alpha_2=\pi/4$ and the right curves for the asymmetrical conditions $a_1=\sqrt{2/3}$, $a_2=\sqrt{1/3}$, $b_1=\sqrt{7/8}$, $b_2=\sqrt{1/8}$, $\alpha_1=\pi/2$, $\alpha_2=\pi/4$. Furthermore, we consider $w_1=w_2=0.5$, $\phi_1=\phi_2=\pi/2$ and the values of dissipation parameter $\tilde{\gamma}$ as the same as considered in Fig. 2.

3.3. The von Neumann entropy for the initial pure and mixed states

Now, we investigate the entanglement between each qubit A, B or C with other parts of the system using the von Neumann entropy which is defined as

$$S^{\rm i}(t)=-{\rm tr}(\hat{\rho}^{\rm i}\ln\hat{\rho}^{\rm i})=-\sum_{\ell}\xi_\ell\ln\xi_\ell, \quad (33)$$

where $\hat{\rho}^{\rm i}$ is the reduced density matrix for the i-th subsystem ($i={\rm A,B,C}$) and correspondingly, ξ_k are the associated with eigenvalues of $\hat{\rho}^{\rm i}$. The reduced density matrices are obtained as follows:

$$\hat{\rho}^{\rm i}={\rm tr}_j\left({\rm tr}_k(\tilde{\hat{\rho}})\right)=\frac{1}{\mathcal{N}(t)}\begin{pmatrix}\rho^{\rm i}_{11} & \rho^{\rm i}_{12}\\ \rho^{\rm i}_{21} & \rho^{\rm i}_{22}\end{pmatrix},$$
$$i\neq j\neq k={\rm A,B,C}, \quad (34)$$

where $\mathcal{N}(t)$ is the normalization factor that can be obtained according to Eqs. (12), (13) and (29) for the initial W- and GHZ-state as well as a mixed state, respectively. For the initial W-state the relevant matrix elements read

$$\rho^{\rm A}_{11} = -(b^2+a^2)U_{12}^2(t)+a^2U_{11}^2(t),$$
$$\rho^{\rm A}_{22} = (b^2+c^2)U_{22}^2(t)-a^2U_{12}^2(t)$$
$$\rho^{\rm A}_{12} = -\rho^{\rm A}_{21}=(b^2+c^2)U_{22}(t)U_{12}(t)-a^2U_{11}(t)U_{12}(t), \quad (35)$$
$$\rho^{\rm B}_{11} = -b^2U_{12}^2(t)+b^2U_{22}^2(t),$$
$$\rho^{\rm B}_{22} = a^2U_{11}^2(t)-(a^2+c^2)U_{12}^2(t)+c^2U_{22}^2(t),$$
$$\rho^{\rm B}_{12} = -\rho^{\rm B}_{21}=abU_{12}(t)\left(U_{11}(t)-U_{22}(t)\right), \quad (36)$$
$$\rho^{\rm C}_{11} = -c^2U_{12}^2(t)+c^2U_{22}^2(t),$$
$$\rho^{\rm C}_{22} = a^2U_{11}^2(t)-(a^2+b^2)U_{12}^2(t)+b^2U_{22}^2(t),$$
$$\rho^{\rm C}_{12} = -\rho^{\rm C}_{21}=acU_{12}(t)\left(U_{11}(t))-U_{22}(t)\right). \quad (37)$$

Similarly, for GHZ-state one has

$$
\begin{aligned}
\rho_{11}^{\mathrm{A}} &= \left(\lambda_4^2+\lambda_3^2+\lambda_2^2+\lambda_1^2\right)U_{11}^2(t)-2\mathrm{i}\lambda_0\lambda_1\sin\phi U_{11}(t)U_{12}(t)-\lambda_0^2U_{12}^2(t),\\
\rho_{22}^{\mathrm{A}} &= -\left(\lambda_4^2+\lambda_3^2+\lambda_2^2+\lambda_1^2\right)U_{12}^2(t)+2\mathrm{i}\lambda_0\lambda_1\sin\phi U_{12}(t)U_{22}(t)+\lambda_0^2U_{22}^2(t),\\
\rho_{12}^{\mathrm{A}} &= (\rho_{21}^{\mathrm{A}})^* = -\left(\lambda_4^2+\lambda_3^2+\lambda_2^2+\lambda_1^2\right)U_{11}(t)U_{12}(t)-\mathrm{e}^{-\mathrm{i}\phi}\lambda_0\lambda_1U_{12}^2(t)+\mathrm{e}^{i\phi}\lambda_0\lambda_1U_{11}(t)U_{22}(t)+\lambda_0^2U_{12}(t)U_{22}(t), \qquad (38)\\
\rho_{11}^{\mathrm{B}} &= \left(\lambda_4^2+\lambda_3^2\right)\left(U_{11}^2(t)-U_{12}^2(t)\right),\\
\rho_{22}^{\mathrm{B}} &= \left(\lambda_2^2+\lambda_1^2\right)U_{11}^2(t)-\left(\lambda_2^2+\lambda_1^2+\lambda_0^2\right)U_{12}^2(t)+2\mathrm{i}\lambda_0\lambda_1\sin\phi U_{12}(t)\left(U_{22}(t)-U_{11}(t)\right),\\
\rho_{12}^{\mathrm{B}} &= (\rho_{21}^{\mathrm{B}})^* = \left(\lambda_2\lambda_4+\mathrm{e}^{-\mathrm{i}\phi}\lambda_1\lambda_3\right)U_{11}^2(t)-\left(\lambda_2\lambda_4+\mathrm{e}^{-\mathrm{i}\phi}\lambda_1\lambda_3\right)U_{12}^2(t)+\lambda_0\lambda_3U_{12}(t)\left(U_{22}(t)-U_{11}(t)\right), \qquad (39)\\
\rho_{11}^{\mathrm{C}} &= \left(\lambda_4^2+\lambda_2^2\right)\left(U_{11}^2(t)-U_{12}^2(t)\right),\\
\rho_{22}^{\mathrm{C}} &= \left(\lambda_3^2+\lambda_1^2\right)U_{11}^2(t)-\left(\lambda_3^2+\lambda_1^2+\lambda_0^2\right)U_{12}^2(t)+2\mathrm{i}\lambda_0\lambda_1\sin\phi U_{12}(t)\left(U_{22}(t)-U_{11}(t)\right),\\
\rho_{12}^{\mathrm{C}} &= (\rho_{21}^{\mathrm{C}})^* = \left(\lambda_3\lambda_4+\mathrm{e}^{-\mathrm{i}\phi}\lambda_1\lambda_2\right)\left(U_{11}^2(t)-U_{12}^2(t)\right)+\lambda_0\lambda_2U_{12}(t)\left(U_{22}(t)-U_{11}(t)\right), \qquad (40)
\end{aligned}
$$

and for the mixed initial state one has

$$
\begin{aligned}
\rho_{11}^{\mathrm{A}} &= w_1\left(-b_1^2U_{12}^2(t)+a_1^2U_{11}^2(t)\right)+w_2\left(-b_2^2U_{12}^2(t)+a_2^2U_{11}^2(t)\right),\\
\rho_{22}^{\mathrm{A}} &= w_1\left(b_1^2U_{22}^2(t)-a_1^2U_{12}^2(t)\right)+w_2\left(b_2^2U_{22}^2(t)-a_2^2U_{12}^2(t)\right),\\
\rho_{12}^{\mathrm{A}} &= -\rho_{21}^{\mathrm{A}} = w_1U_{12}(t)\left(b_1^2U_{22}(t)-a_1^2U_{11}(t)\right)+w_2U_{12}(t)\left(b_2^2U_{22}(t)-a_2^2U_{11}(t)\right), \qquad (41)\\
\rho_{11}^{\mathrm{B}} &= w_1b_1^2\left(U_{22}^2(t)-U_{12}^2(t)\right)+w_2\sin^2\alpha_2\left(a_2^2(U_{11}^2(t)-U_{12}^2(t))+b_2^2(U_{22}^2(t)-U_{12}^2(t))\right),\\
\rho_{22}^{\mathrm{B}} &= w_1a_1^2\left(U_{11}^2(t)-U_{12}^2(t)\right)+w_2\cos^2\alpha_2\left(a_2^2(U_{11}^2(t)-U_{12}^2(t))+b_2^2(U_{22}^2(t)-U_{12}^2(t))\right),\\
\rho_{12}^{\mathrm{B}} &= -\rho_{21}^{1\mathrm{B}} = -w_1a_1b_1U_{12}(t)(U_{22}(t)-U_{11}(t))+w_2\sin\alpha_2\cos\alpha_2\,\mathrm{e}^{-\mathrm{i}\phi_2}\left(a_2^2(U_{11}^2(t)-U_{12}^2(t))+b_2^2(U_{22}^2(t)-U_{12}^2(t))\right), \qquad (42)\\
\rho_{11}^{\mathrm{C}} &= w_1\sin^2\alpha_1\left(a_1^2\left(U_{11}^2(t)-U_{12}^2(t)\right)+b_1^2\left(U_{22}^2(t)-U_{12}^2(t)\right)\right)+w_2b_2^2\left(U_{22}^2(t)-U_{12}^2(t)\right),\\
\rho_{22}^{\mathrm{C}} &= w_1\cos^2\alpha_1\left(a_1^2\left(U_{11}^2(t)-U_{12}^2(t)\right)+b_1^2\left(U_{22}^2(t)-U_{12}^2(t)\right)\right)+w2a_2^2\left(U_{11}^2(t)-U_{12}^2(t)\right),\\
\rho_{12}^{\mathrm{C}} &= -\rho_{21}^{\mathrm{C}} = w_1\sin\alpha_1\cos\alpha_1\,\mathrm{e}^{-\mathrm{i}\phi_1}\left(a_1^2\left(U_{11}^2(t)-U_{12}^2(t)\right)+b_1^2\left(U_{22}^2(t)-U_{12}^2(t)\right)\right)-w_2a_2b_2U_{12}(t)\left(U_2(t)-U_{11}(t)\right). \qquad (43)
\end{aligned}
$$

We plot the von Neumann entropy (Eq. (33)) for the initial pure W-(GHZ-) state and for the initial mixed state, respectively, in Figs. 5–7. The von Neumann entropy corresponding to qubits B and C leads to the same results for the symmetrical initial conditions, as seen in the left curves in Figs. 5 and 6 for the initial W and GHZ states, respectively. In more detail, for instance, $S_{\mathrm{W}}^{\mathrm{A}}(t)$ shows the entanglement between the qubit A and all other subsystems constituting our considered model, i.e., qubits B, C, and the environment, when the initial state is W-state. Similar interpretations may be given for other plots shown in Figs. 5–7. As may be observed, in all cases the entanglement is revealed, however, in different manners; i.e., oscillatory, non-oscillatory decaying and also death and alive of the entanglement in some periods of scaled time. Interestingly, in this case also the von Neumann entropy for the considered model behaves as the Morkovian (non-Markovian) regime for $\tilde{\gamma}>1$ ($\tilde{\gamma}<1$).

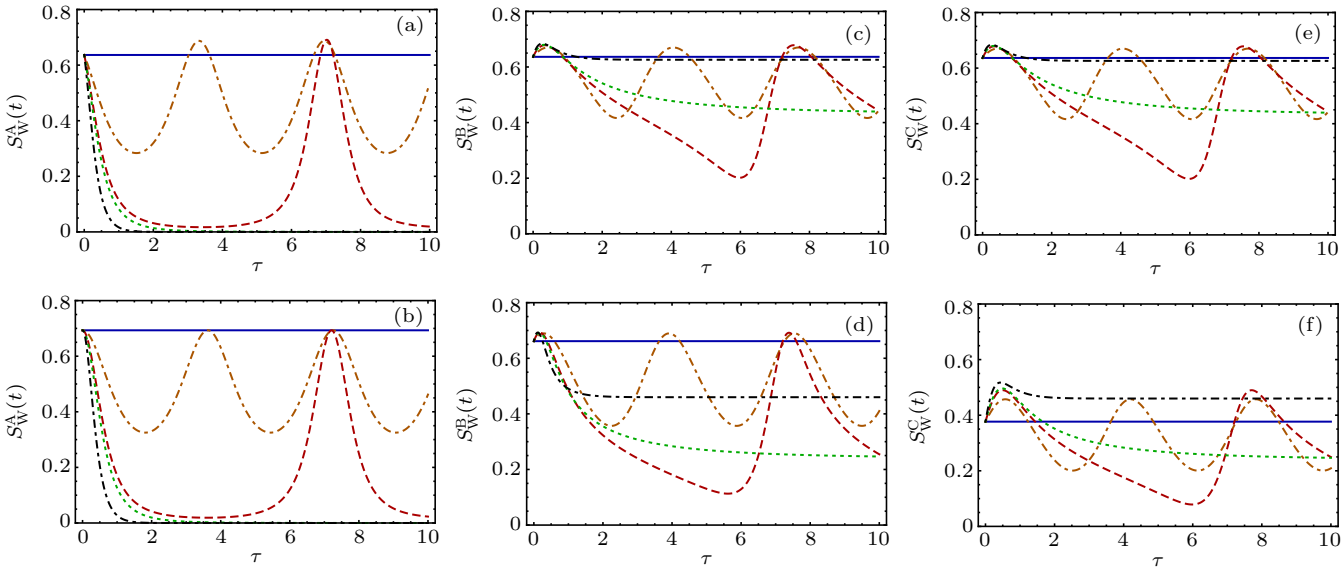


Fig. 5. The von Neumann entropy against scaled time $\tau=\Delta t$ for the initial W-state. The entropy $S_{\mathrm{W}}^{\mathrm{A}}(t)$, $S_{\mathrm{W}}^{\mathrm{B}}(t)$ and $S_{\mathrm{W}}^{\mathrm{C}}(t)$ are plotted in the subspecies [(a), (b), [(c), (d)],and [(e), (f)], respectively. We plot the upper curves for the symmetrical initial conditions $a=b=c=\sqrt{1/3}$ and the lower curves for the asymmetrical conditions $a=\sqrt{1/2}$, $b=\sqrt{3/8}$, $c=\sqrt{1/8}$. Furthermore, we consider the values of $\tilde{\gamma}$ as same as those in Fig. 2.

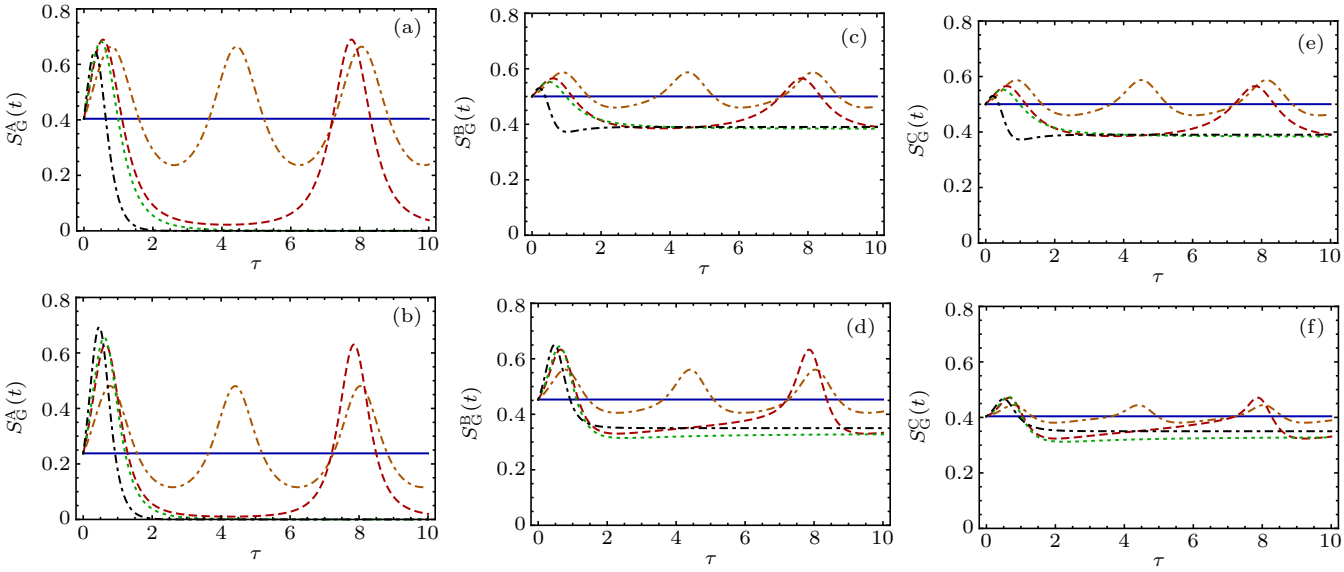


Fig. 6. The von Neumann entropy against scaled time $\tau = \Delta t$ for the initial GHZ-state. The entropies $S_G^A(t)$, $S_G^B(t)$ and $S_G^C(t)$ are plotted in the subspecies [(a), (b)], [(c), (d)], and [(e), (f)], respectively. We plot the upper curves for the symmetrical initial conditions $\lambda_0 = \lambda_1 = \lambda_2 = \lambda_3 = \lambda_4 = 1/\sqrt{5}$ and the lower curves for the asymmetrical conditions $\lambda_0 = \sqrt{0.1}$, $\lambda_1 = \sqrt{0.3}$, $\lambda_2 = \sqrt{0.1}$, $\lambda_3 = \sqrt{0.3}$, $\lambda_4 = \sqrt{0.2}$. Furthermore, we consider $\phi = \pi/2$ and the values of $\tilde{\gamma}$ as same as those in Fig. 2.

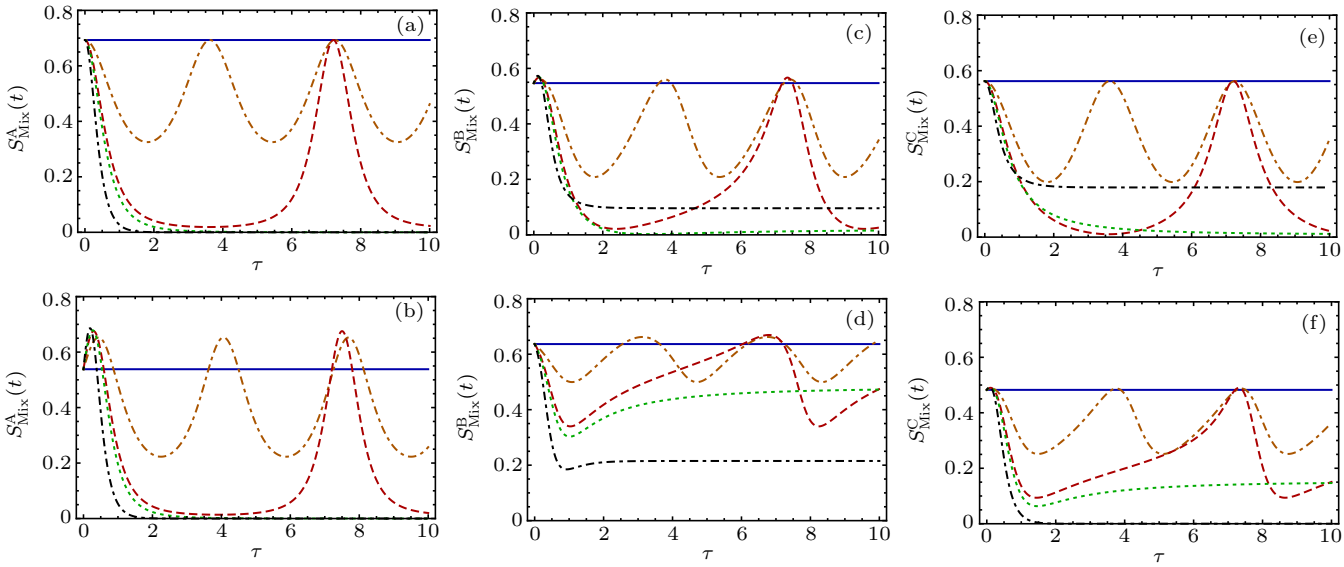


Fig. 7. The von Neumann entropy against scaled time $\tau = \Delta t$ for the initial mixed state. The entropies $S_{Mix}^A(t)$, $S_{Mix}^B(t)$ and $S_{Mix}^C(t)$ are plotted in the subspecies [(a), (b)], [(c), (d)], and [(e), (f)], respectively. We plot the upper curves for the symmetrical initial conditions $a_1 = a_2 = b_1 = b_2 = 1/\sqrt{2}$, $\alpha_1 = \alpha_2 = \pi/4$ and the lower curves for the asymmetrical conditions $a_1 = \sqrt{2/3}$, $a_2 = \sqrt{1/3}$, $b_1 = \sqrt{7/8}$, $b_2 = \sqrt{1/8}$, $\alpha_1 = \pi/2$, $\alpha_2 = \pi/4$. Furthermore, we consider $w_1 = w_2 = 0.5$, $\phi_1 = \phi_2 = \pi/2$ and the values of dissipation parameter $\tilde{\gamma}$ as same as considered in Fig. 2.

4. Summary and conclusions

We have used the non-Hermitian Hamiltonian approach to study the dynamical behavior of entanglement between each pairs of three entangled qubits (only one of the qubits interacts with its environment) in the presence of dissipation. For this purpose, we obtain the time evolution of the density matrix after applying the time evolution operator on the pure as well as mixed initial density matrices associated with the three qubits. Then, we calculate the reduced density matrix corresponding to each pair of qubits and subsequently we evaluate the concurrence measure and von Neumann entropy, numerically. In general, comparing to Ref. [25], we have generalized the presented model given in Ref. [25] in two aspects: (i) We have extended the model in Ref. [25] to three qubits which are initially prepared in pure and mixed entangled state (one of the qubits affected by environment and the other two qubits are isolated from the environment) instead of only two (initially entangled) qubits (one affected by environment and the other qubit is isolated in Ref. [25]). (ii) Also, we investigate the entanglement between qubit pairs by concurrence measure while in Ref. [25], the entanglement has been studied by the inappropriate measure. Indeed, we have investigated the influences of dissipation parameter on the entanglement of various pairs of qubits via the concurrence which is the most suitable

measure for two qubit systems. Our numerical results for the pure and mixed initial states show that the concurrence and von Neumann entropy do not change for $\tilde{\gamma}=0$, demonstrating the stability of entanglement between qubits in the absence of dissipation. Furthermore, the entanglement in two pairs of initially entangled qubits AB and AC monotonically decreases with increasing the strength of dissipation. This behavior has been characterized before for the Markovian regimes. Moreover, for $\tilde{\gamma}<1$, some oscillations may be observed in the above mentioned subsystems which can correspond to the non-Markovian regimes. Thus, we may define $\tilde{\gamma}=1$ as the critical dissipative value in our non-Hermitian approach, in which by controlling it one can arrive at a Markovian or non-Markovian regime. Also, for the entanglement between the pair BC, we observe that for the pure state the qubits B and C which have been initially isolated from the environment become entangled, while for initial mixed states this pair remains separable as time goes on. It is interesting to notice that the entanglement stability grows to values more than its initial value in the pair qubit BC for the pure state. Similarly, the evolution of the von Neumann entropy of qubits A, B and C are consistent with the Markovian and non-Markovian regimes for $\tilde{\gamma}>1$ and $\tilde{\gamma}<1$, respectively.

Appendix A

The reduced density transformed matrix $\hat{\rho}_{\rm red}^{\rm AB}$ for the GHZ-state and mixed initial density matrix can be written as

$$\hat{\rho}_{\rm red}^{\rm AB}=\frac{1}{\mathcal{N}(t)}\begin{pmatrix}\rho_{11}^{\rm AB}&\rho_{12}^{\rm AB}&\rho_{13}^{\rm AB}&\rho_{14}^{\rm AB}\\ \rho_{21}^{\rm AB}&\rho_{22}^{\rm AB}&\rho_{23}^{\rm AB}&\rho_{24}^{\rm AB}\\ \rho_{31}^{\rm AB}&\rho_{32}^{\rm AB}&\rho_{33}^{\rm AB}&\rho_{34}^{\rm AB}\\ \rho_{41}^{\rm AB}&\rho_{42}^{\rm AB}&\rho_{43}^{\rm AB}&\rho_{44}^{\rm AB}\end{pmatrix},$$

where $\mathcal{N}(t)$ is the normalization factor defined in Eqs. (13) and (29), corresponding to GHZ-state and mixed state, respectively. The matrix elements for GHZ-state may be obtained as follows:

$$\begin{aligned}
\rho_{11}^{\rm AB} &= \left(\lambda_3^2+\lambda_4^2\right)U_{11}^2(t),\ \rho_{22}^{\rm AB}=-\left(\lambda_3^2+\lambda_4^2\right)U_{12}^2(t),\quad \rho_{33}^{\rm AB}=\left(\lambda_1^2+\lambda_2^2\right)U_{11}^2(t)-2{\rm i}\sin\phi\lambda_0\lambda_1U_{11}(t)U_{12}(t)-\lambda_0^2U_{12}^2(t),\\
\rho_{44}^{\rm AB} &= -\left(\lambda_1^2+\lambda_2^2\right)U_{12}^2(t)+2{\rm i}\sin\phi\lambda_0\lambda_1U_{12}(t)U_{22}(t)+\lambda_0^2U_{22}^2(t),\quad \rho_{12}^{\rm AB}=-\rho_{21}^{\rm AB}=-\left(\lambda_3^2+\lambda_4^2\right)U_{11}(t)U_{12}(t),\\
\rho_{13}^{\rm AB} &= \left(\rho_{31}^{\rm AB}\right)^*=\left(\lambda_2\lambda_4+{\rm e}^{-{\rm i}\phi}\lambda_1\lambda_3\right)U_{11}^2(t)-\lambda_0\lambda_3U_{11}(t)U_{12}(t),\\
\rho_{14}^{\rm AB} &= \left(\rho_{41}^{\rm AB}\right)^*=-\left(\lambda_2\lambda_4+{\rm e}^{-{\rm i}\phi}\lambda_1\lambda_3\right)U_{11}(t)U_{12}(t)+\lambda_0\lambda_3U_{12}(t)U_{22}(t),
\end{aligned}$$

and also, the matrix elements for the mixed initial state read

$$\begin{aligned}
\rho_{23}^{\rm AB} &= \left(\rho_{32}^{\rm AB}\right)^*=\left(\lambda_2\lambda_4+{\rm e}^{-{\rm i}\phi}\lambda_1\lambda_3\right)U_{11}(t)U_{12}(t)-\lambda_0\lambda_3U_{12}^2(t),\\
\rho_{24}^{\rm AB} &= \left(\rho_{42}^{\rm AB}\right)^*=-\left(\lambda_2\lambda_4+{\rm e}^{-{\rm i}\phi}\lambda_1\lambda_3\right)U_{12}^2(t)+\lambda_0\lambda_3U_{12}(t)U_{22}(t),\\
\rho_{34}^{\rm AB} &= \left(\rho_{43}^{\rm AB}\right)^*=-\left(\lambda_1^2+\lambda_2^2\right)U_{11}(t)U_{12}(t)+{\rm e}^{-{\rm i}\phi}\lambda_0\lambda_1U_{12}^2(t)+\left(\lambda_0\lambda_1{\rm e}^{{\rm i}\phi}U_{11}(t)+\lambda_0^2U_{12}(t)\right)U_{22}(t),\\
\rho_{11}^{\rm AB} &= w_2a_2^2\sin^2\alpha_2U_{11}^2(t)-w_1b_1^2U_{12}^2(t)-w_2b_2^2\sin^2\alpha_2U_{12}^2(t),\\
\rho_{22}^{\rm AB} &= -w_2a_2^2\sin^2\alpha_2U_{12}^2(t)+w_1b_1^2U_{22}^2(t)+w_2b_2^2\sin^2\alpha_2U_{22}^2(t),\\
\rho_{33}^{\rm AB} &= w_2a_2^2\cos^2\alpha_2+w_1a_1^2U_{11}^2(t)-w_2a_2^2\cos^2\alpha_2U_{12}^2(t),\\
\rho_{44}^{\rm AB} &= -w_2a_2^2\cos^2\alpha_2-w_1a_1^2U_{12}^2(t)+w_2b_2^2\cos^2\alpha_2U_{22}^2(t),\\
\rho_{12}^{\rm AB} &= -\rho_{21}^{\rm AB}=-w_2a_2^2\sin\alpha_2^2U_{11}(t)U_{12}(t)+w_1b_1^2\cos\alpha_1^2U_{12}(t)U_{22}(t)+(w_2b_2^2\sin\alpha_2^2+w_1b_1^2\sin^2\alpha_2)U_{12}(t)U_{22}(t),\\
\rho_{13}^{\rm AB} &= w_1a_1b_1\sin^2\alpha_1U_{11}(t)U_{12}(t)-w_2b_2^2{\rm e}^{-{\rm i}\phi_2}\cos\alpha_2\sin\alpha_2U_{12}(t)^2(t)\\
&\quad +U_{11}(t)\left[w_2a_2^2{\rm e}^{-{\rm i}\phi_2}\cos\alpha_2\sin\alpha_2U_{11}(t)+w_1a_1b_1\cos\alpha_1^2U_{12}(t)\right],\\
\rho_{31}^{\rm AB} &= -w_1a_1b_1\sin^2\alpha_1U_{11}(t)U_{12}(t)-w_2b_2^2{\rm e}^{{\rm i}\phi_2}\cos\alpha_2\sin\alpha_2U_{12}(t)^2(t)\\
&\quad +U_{11}(t)\left[w_2a_2^2{\rm e}^{{\rm i}\phi_2}\cos\alpha_2\sin\alpha_2U_{11}(t)-w_1a_1b_1\cos\alpha_1^2U_{12}(t)\right],\\
\rho_{14}^{\rm AB} &= -w_1a_1b_1\sin^2\alpha_1U_{12}^2(t)-w_2U_{12}(t)\left[a_2^2{\rm e}^{-{\rm i}\phi_2}\cos\alpha_2\sin\alpha_2U_{11}(t)\right.\\
&\quad \left.+w_1a_1b_1\cos^2\alpha_1U_{12}(t)\right]+w_2b_2^2{\rm e}^{-{\rm i}\phi_2}\cos\alpha_2\sin\alpha_2U_{12}(t)U_{22}(t),\\
\rho_{41}^{\rm AB} &= -w_1a_1b_1\sin^2\alpha_1U_{12}^2(t)+w_2U_{12}(t)\left[a_2^2{\rm e}^{{\rm i}\phi_2}\cos\alpha_2\sin\alpha_2U_{11}(t)\right.\\
&\quad \left.-w_1a_1b_1\cos^2\alpha_1U_{12}(t)\right]-w_2b_2^2{\rm e}^{{\rm i}\phi_2}\cos\alpha_2\sin\alpha_2U_{12}(t)U_{22}(t),\\
\rho_{23}^{\rm AB} &= w_1a_1b_1\sin^2\alpha_1U_{11}(t)U_{12}(t)-w_2b_2^2{\rm e}^{-{\rm i}\phi_2}\cos\alpha_2\sin\alpha_2U_{12}(t)U_{22}(t)\\
&\quad +U_{11}(t)\left[w_2a_2^2{\rm e}^{-{\rm i}\phi_2}\cos\alpha_2\sin\alpha_2U_{12}(t)+w_1a_1b_1\cos^2\alpha_1U_{22}(t)\right],\\
\rho_{32}^{\rm AB} &= -w_1a_1b_1\sin^2\alpha_1U_{11}(t)U_{12}(t)+w_2b_2^2{\rm e}^{{\rm i}\phi_2}\cos\alpha_2\sin\alpha_2U_{12}(t)U_{22}(t)
\end{aligned}$$

$$
\begin{aligned}
&+U_{11}(t)\left[-w_2a_2^2\,\mathrm{e}^{\mathrm{i}\phi_2}\cos\alpha_2\sin\alpha_2U_{12}(t)+w_1a_1b_1\cos^2\alpha_1U_{22}(t)\right],\\
\rho_{24}^{\mathrm{AB}} &= -w_1a_1b_1\sin^2\alpha_1U_{12}(t)U_{22}(t)+w_2b_2^2\,\mathrm{e}^{-\mathrm{i}\phi_2}\cos\alpha_2\sin\alpha_2U_{22}^2(t)\\
&\quad -U_{12}(t)\left[w_2a_2^2\,\mathrm{e}^{-\mathrm{i}\phi_2}\cos\alpha_2\sin\alpha_2U_{12}(t)+w_1a_1b_1\cos^2\alpha_1U_{22}(t)\right],\\
\rho_{42}^{\mathrm{AB}} &= w_1a_1b_1\sin^2\alpha_1U_{12}(t)U_{22}(t)+w_2b_2^2\,\mathrm{e}^{\mathrm{i}\phi_2}\cos\alpha_2\sin\alpha_2U_{22}^2(t)\\
&\quad +U_{12}(t)\left[-w_2a_2^2\,\mathrm{e}^{\mathrm{i}\phi_2}\cos\alpha_2\sin\alpha_2U_{12}(t)+w_1a_1b_1\cos^2\alpha_1U_{22}(t)\right],\\
\rho_{34}^{\mathrm{AB}} &= -\rho_{43}^{\mathrm{AB}}=(-w_2a_2^2\cos^2\alpha_2-w_1a_1^2\cos^2\alpha_2)U_{11}(t)U_{12}(t)-w_1a_1^2\sin^2\alpha_1U_{11}(t)U_{12}(t)+w_2b_2^2\cos\alpha_2^2U_{12}(t)U_{22}(t).
\end{aligned}
$$

References

[1] Bennett C H, Brassard G, Crépeau C, Jozsa R, Peres A and Wootters W K 1993 *Phys. Rev. Lett.* **70** 1895
[2] Wang X, Sanders B C and Berry D W 2003 *Phys. Rev. A* **67** 042323
[3] Zhou Y Y, Li P F, Yan Z H and Jia X J 2019 *Acta. Phys. Sin.* **68** 234203 (in Chinese)
[4] Amazioug M, Jebli L, Nassik M and Habiballah N 2020 *Chin. Phys. B* **29** 020304
[5] Lu L C, Wang G Y, Ren B C, Zhang M and Deng F G 2020 *Chin. Phys. B* **29** 010305
[6] Breuer H P and Petruccione F 2002 *The Theory of Open Quantum Systems* (Oxford: Oxford University Press)
[7] Scully M O and Zubairy M S 1997 *Quantum Optics* (Cambridge: Cambridge University Press)
[8] Leggett A J, Chakravarty S, Dorsey, A T, Fisher Matthew P, Garg A and Zwerger W 1987 *Rev. Mod. Phys.* **59** 1
[9] Bellomo B, Franco R L and Compagno G 2007 *Phys. Rev. Lett.* **99** 160502
[10] Lu X M, Wang X and Sun C P 2010 *Phys. Rev. A* **82** 042103
[11] Zhong W, Sun Z, Ma J, Wang X and Nori F 2013 *Phys. Rev. A* **87** 022337
[12] Tan J, Kyaw T H and Yeo Y 2010 *Phys. Rev. A* **81** 062119
[13] Breuer H P, Laine E M, Piilo J and Vacchini B 2016 *Rev. Mod. Phys.* **88** 021002
[14] Fan Z L, Ren Y K and Zeng H S 2016 *Chin. Phys. B* **25** 010303
[15] Mu Q and Lin P 2020 *Chin. Phys. B* **29** 060304
[16] Nourmandipour A, Tavassoly M K and Rafiee M 2016 *Phys. Rev. A* **93** 022327
[17] Marshall J, Venuti L C and Zanardi P 2017 *Phys. Rev. A* **96** 052113
[18] Golkar S and Tavassoly M K 2018 *Chin. Phys. B* **27** 040303
[19] Ban M, Kitajima S and Shibata F 2005 *J. Phys. A* **38** 7161
[20] Yu T and Eberly J H 2007 *Quantum Inform. Comput.* **7** 459
[21] Bagarell F, Lattuca M, Passante R, Rizzuto L and Spagnolo S 2015 *Phys. Rev. A* **91** 042134
[22] Sergi A and Zloshchastiev K G 2013 *Int. J. Mod. Phys. B* **27** 1345053
[23] Sergi A and Zloshchastiev K G 2016 *J. Stat. Mech.* **2016** 033102
[24] Sergi A and Giaquinta P V 2016 *Entropy* **18** 451
[25] Zhang S Y, Fang M F and Xu L 2017 *Quant. Inf. Proc.* **16** 234
[26] Wang Y Y and Fang M F 2020 *Chin. Phys. B* **29** 030304
[27] Dong Y, Zhang W J, Liu J and Xie X T 2019 *Chin. Phys. B* **28** 114202
[28] He Z, Nie Z Y and Wang Q 2019 *Chin. Phys. B* **28** 120305
[29] Huang Y, Xiong H N, Zhong W, Hu Z D and Ye E J 2016 *Europhys. Lett.* **114** 20002
[30] Mirza Imran M, van Enk, S J and Kimble H J 2013 *J. Opt. Soc. Am. B* **30** 2640
[31] Guo J L and Wei J L 2015 *Ann. Phys.* **354** 522
[32] Ma P C, Chen G B, Li X W and Zhan Y B 2016 *Laser Phys.* **26** 105201
[33] Arthur T T and Fai M C 2017 *Quant. Inf. Proc.* **17** 136
[34] Behzadi N, Ahansaz B and Faizi E 2017 *Eur. Phys. J. D* **71** 280
[35] Neergaard Nielsen J S, Nielsen B M, Hettich C, Molmer K and Polzik E S 2006 *Phys. Rev. Lett.* **97** 083604
[36] Prevedel R, Gronenberg G, Tame M S, Paternosto M, Walther P, Kim M S and Zeilinger A 2009 *Phys. Rev. Lett.* **103** 020503
[37] DiCarlo L, Reed M D, Sun L, Johnson B R, Chow J M, Gambetta J M, Frunzio L, Girvin S M, Devoret M H and Schoelkopf R J 2010 *Nature* **467** 574
[38] Zhao C, Zhu M and Ye L 2011 *J. Opt. Soc. Am. B* **28** 1740
[39] Zhang Y h and Xia Y j 2015 *Laser Phys.* **25** 055201
[40] Wang X W, Yu S, Zhang D Y and Oh C H 2016 *Sci. Rep.* **6** 22408
[41] Häffner H, Hänsel W, Roos C F, Benhelm J, Chek-al-kar D, Chwalla M, Käber T, Rapol U D, Riebe M, Schmidt P O, Becher C, Gähe O, Dür W and Blatt R 2005 *Nature* **438** 643
[42] Dür W, Vidal G and Cirac J I 2000 *Phys. Rev. A* **62** 062314
[43] Acín A, Andrianov A, Costa L, Jané E, Latorre J I and Tarrach R 2000 *Phys. Rev. Lett.* **85** 1560
[44] Acín A, Bruß D, Lewenstein M, and Sanpera A 2001 *Phys. Rev. Lett.* **87** 040401
[45] Wootters W K 2001 *Quantum Inform. Comput.* **1** 27
[46] Li J G, Zou J and Shao B 2010 *Phys. Rev. A* **82** 042318
[47] Tong Q J, An J H, Luo H G and Oh C H 2010 *Phys. Rev. A* **81** 052330
[48] Zhou J, Wu C, Zhu M and Guo H 2009 *J. Phys. B: At. Mol. Opt. Phys.* **42** 215505
[49] Golkar S and Tavassoly M K 2018 *Laser Phys. Lett.* **15** 035205
[50] Lopez C E, Romero G, Lastra F, Solano E and Retamal J C 2008 *Phys. Rev. Lett.* **101** 080503